nature immunology

Recognition of CD1d-sulfatide mediated by a type II natural killer T cell antigen receptor

Onisha Patel[1,7], Daniel G Pellicci[2,7], Stephanie Gras[1,7], Maria L Sandoval-Romero[1], Adam P Uldrich[2], Thierry Mallevaey[3,6], Andrew J Clarke[1], Jérôme Le Nours[1], Alex Theodossis[1], Susanna L Cardell[4], Laurent Gapin[3], Dale I Godfrey[2,8] & Jamie Rossjohn[1,5,8]

Natural killer T cells (NKT cells) are divided into type I and type II subsets on the basis of differences in their T cell antigen receptor (TCR) repertoire and CD1d-antigen specificity. Although the mode by which type I NKT cell TCRs recognize CD1d-antigen has been established, how type II NKT cell TCRs engage CD1d-antigen is unknown. Here we provide a basis for how a type II NKT cell TCR, XV19, recognized CD1d-sulfatide. The XV19 TCR bound orthogonally above the A′ pocket of CD1d, in contrast to the parallel docking of type I NKT cell TCRs over the F′ pocket of CD1d. At the XV19 TCR–CD1d-sulfatide interface, the TCRα and TCRβ chains sat centrally on CD1d, where the malleable CDR3 loops dominated interactions with CD1d-sulfatide. Accordingly, we highlight the diverse mechanisms by which NKT cell TCRs can bind CD1d and account for the distinct antigen specificity of type II NKT cells.

Natural killer T cells (NKT cells) specifically recognize self lipid–based or foreign lipid–based antigens bound to the antigen-presenting molecule CD1d[1]. There are two broad classes of NKT cells: type I and type II. Type I NKT cells (semi-invariant NKT cells) are defined by expression of an invariant T cell antigen receptor (TCR) α-chain (α-chain variable region 24–α-chain joining region 18 ($V_α$24-$J_α$18) in humans; $V_α$14-$J_α$18 in mice) paired with a limited repertoire of TCRβ chains ($V_β$11 in humans; $V_β$8, $V_β$7 and $V_β$2 in mice) and by their ability to recognize the non-self glycolipid antigen α-galactosylceramide (α-GalCer)[1]. In contrast, type II NKT cells express a different and more diverse TCR repertoire. When activated, NKT cells produce an array of cytokines of the T_H1, T_H2 and T_H17 subsets of helper T cell responses, which enables them to influence the immunological outcomes of a broad range of diseases[1]. Some reports have indicated that type I and type II NKT cells may have distinct and possibly opposing functions. For example, type I NKT cells typically promote tumor rejection in mice, whereas type II NKT cells seem to suppress it[2]. Given the potentially different functions of type I and type II NKT cells, it is important to understand the molecular basis for the diverse antigen specificity of the two cell types.

The structures of human and mouse type I NKT cell TCRs have been determined in complex with CD1d loaded with a variety of lipid-based antigens from synthetic, self and microbial sources[3–9]. The lipid tails sit in the A′ and F′ pockets of CD1d, whereas the polar head groups protrude and are contacted by the NKT cell TCR. Collectively, these type I NKT cell TCR–CD1d-antigen complexes have a highly conserved docking strategy whereby the type I NKT cell TCR sits parallel over the F′ pocket of CD1d, which suggests that the type I NKT cell TCR is akin to an innate-like pattern-recognition receptor[10]. In this common footprint, the TCRα chain dominates the interaction, binding to CD1d and the antigen, whereas the TCRβ chain contacts CD1d. Nevertheless, differing contributions from the complementarity-determining region (CDR) α-and β-loops of the type I NKT cell TCR are evident in some CD1d-antigen complexes. For example, the autoreactivity of the type I NKT cell TCR–CD1d complex is associated with CDR3β loop–mediated interactions with CD1d[8,11–13]. Moreover, alterations in the $V_α$ and/or $V_β$ use of the type I NKT cell TCR can affect the specificity for CD1d-restricted antigens. For example, $V_β$8, $V_β$7 and $V_β$2 show different recognition of various analogs of α-GalCer[12,14,15]. Nevertheless, in each case the docking mode is 'fixed' with parallel binding over the F′ pocket of CD1d[5,16]. However it is unclear whether type II NKT cell TCRs engage CD1d-antigen in a similar manner or adopt a distinct docking mode reflecting their different TCR use and antigen specificity.

Although the antigen specificity of type II NKT cells is poorly understood, it is clearly distinct from that of type I NKT cells. Indeed, type II NKT cells are partly defined by their lack of reactivity to CD1d–α-GalCer; instead, these cells recognize a range of distinct lipid-based antigens presented by CD1d[1]. A widely studied antigen for type II NKT cells is sulfatide, a sulfated form of β-galactosylceramide (β-GalCer) that shows enrichment in neuronal tissue; conversely, type I NKT cells are not considered to be sulfatide reactive[17,18].

[1]Department of Biochemistry and Molecular Biology, School of Biomedical Sciences, Monash University, Clayton, Australia. [2]Department of Microbiology & Immunology, University of Melbourne, Parkville, Australia. [3]Department of Immunology, University of Colorado Denver and National Jewish Health, Denver, Colorado, USA. [4]Department of Microbiology and Immunology, Institute of Biomedicine, University of Goteborg, Goteborg, Sweden. [5]Institute of Infection and Immunity, Cardiff University School of Medicine, Cardiff, UK. [6]Present address: Department of Immunology, University of Toronto, Toronto, Canada. [7]These authors contributed equally to this work. [8]These authors jointly directed this work. Correspondence should be addressed to J.R. (jamie.rossjohn@monash.edu) or D.I.G. (godfrey@unimelb.edu.au).

Received 2 April; accepted 11 June; published online 22 July 2012; doi:10.1038/ni.2372

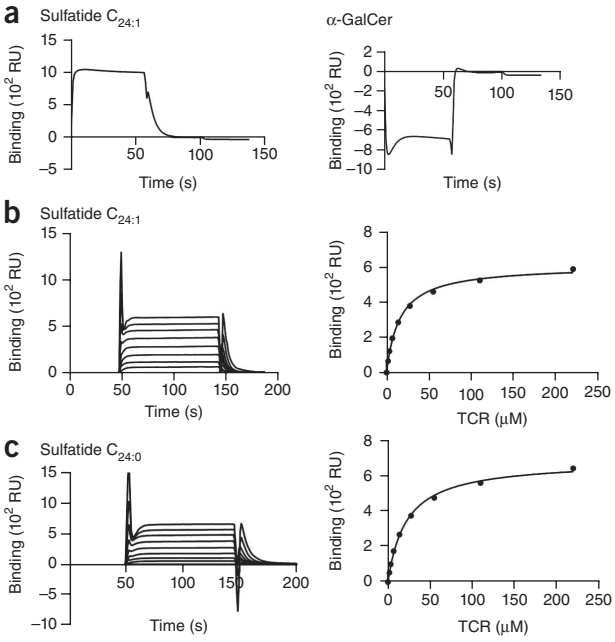

Figure 1 Analysis of the binding of the XV19 TCR to CD1d-sulfatide. (**a**) Binding of the XV19 TCR to CD1d-sulfatide ($C_{24:1}$; left) and to CD1d–α-GalCer (right), a prototypic lipid antigen for type I NKT cell TCRs; results are presented in response units (RU) after subtraction of the response from that of CD1d purified from insect cells with unidentified endogenous antigen (control). The negative results for CD1d–α-GalCer are due to the greater reactivity of XV19 to CD1d plus endogenous antigen. (**b**) Binding of the XV19 TCR to CD1d-sulfatide ($C_{24:1}$; left); results are presented after subtraction of the response obtained with streptavidin-coated chip alone. Right, equilibrium binding-response curve of the binding of increasing concentrations of the XV19 TCR. (**c**) Binding of the XV19 TCR to CD1d-sulfatide ($C_{24:0}$; left); results presented as in **b**. Right, equilibrium binding-response curve (as in **b**). Data are from one of two independent experiments.

Although the type II NKT cell TCR repertoire is considered diverse, some biases in $V_\alpha3$, $V_\alpha8$, $V_\beta3$ and $V_\beta8$ use have been observed[19,20], and a study of sulfatide-reactive type II NKT cells has demonstrated a more highly conserved CDR3β region in these cells than in type I NKT cells[20]. Understanding the antigen specificity of type II NKT cells and, therefore, the immunological function of these cells, is a key step in understanding NKT cell–mediated immunity. Here we describe the molecular basis of how a prototypical sulfatide-reactive type II NKT cell TCR (XV19) engages its ligand CD1d-sulfatide. Notably, in contrast to the docking mode of the canonical type I NKT cell TCR on CD1d-antigen, this type II NKT cell TCR bound orthogonally to and at the extreme end of the A′ pocket of the CD1d antigen-binding cleft.

RESULTS

Type II NKT cell TCR–CD1d-sulfatide affinity

The mouse XV19 hybridoma represents one of the first characterized type II NKT cells[21] and shows reactivity to several isoforms of the mammalian glycolipid antigen sulfatide[17,18]. To investigate the basis of the reactivity of type II NKT cell TCR–CD1d-sulfatide, we cloned and sequenced the XV19 TCR, which showed $V_\alpha1$-$J_\alpha26$–$V_\beta16$-$J_\beta2.1$ segment use with the CDR3α sequence CAASEQNNYAQGLTF and the CDR3β sequence CASSFWGAYAEQFF (**Supplementary Fig. 1**). Accordingly, the V-J-region use of the XV19 NKT cell TCR was completely distinct from the α- and β-chain use of type I NKT cell TCRs and was identical to that described for the type II NKT cell hybridoma Hy19.3 (ref. 21), which confirmed that these were derived from the same original cell line[21].

Next we expressed and refolded the soluble ectodomains of the XV19 TCR. By surface plasmon resonance we measured the affinity of the XV19 TCR for CD1d loaded with either of two antigenic isoforms of sulfatide distinguished by a monounsaturated ($C_{24:1}$) or saturated ($C_{24:0}$) 24-carbon acyl chain and α-GalCer. We included the type I $V_\beta8.2$ NKT cell TCR[15] as a control. Whereas the type I $V_\beta8.2$ NKT cell TCR showed no binding affinity for the CD1d-sulfatide complexes, it bound to CD1d–α-GalCer with a high (nanomolar) affinity, as expected (data not shown). In contrast, the XV19 TCR did not bind CD1d–α-GalCer (**Fig. 1a**) but showed approximately equivalent affinity for the two CD1d-sulfatide antigens $C_{24:1}$ sulfatide and $C_{24:0}$ sulfatide (dissociation constant at equilibrium, 18.0 ± 2.3 μM ($C_{24:1}$) and 24.5 ± 2.5 μM ($C_{24:0}$; mean ± s.e.m. of two experiments); **Fig. 1b**,**c**). This indicated that the different reactivity of the XV19 NKT cell hybridoma to different forms of sulfatide antigens[17] was more attributable to loading and antigen-presentation mechanisms, analogous to the reactivity of type I NKT cells to lipid-based antigens with modifications in their acyl chains[22–25]. The micromolar affinity of the XV19 TCR–CD1d-sulfatide interaction was in contrast to the nanomolar affinity of type I NKT cell TCRs for CD1d–α-GalCer and was more similar to the affinity of autoreactive type I NKT cell TCRs for β-linked self antigens such as β-GalCer and iGb3 (ref. 8) and was also in the range typically associated with the recognition of complexes of peptide and major histocompatibility complex class I by TCRs[26].

XV19 TCR–CD1d-sulfatide complex

To understand how the XV19 TCR recognizes CD1d-sulfatide, we determined the structure of this TCR in the unligated state to a resolution of 1.7 Å and subsequently determined the structure of the XV19 TCR–CD1d-sulfatide ($C_{24:1}$ form) complex to a resolution of 3.1 Å (**Supplementary Table 1**). The electron density corresponding to the unligated XV19 TCR was unambiguous (data not shown). Furthermore, for the ternary complex, initial experimental phases showed distinct unbiased density for the sulfatide in the CD1d cleft (**Supplementary Fig. 2a**). Although the ternary complex was at medium resolution (3.1 Å), the very-high-resolution structures of the unligated counterparts[27] enabled the ternary complex to be well refined (**Supplementary Table 1**), and the electron density at the XV19 TCR–CD1d-sulfatide interface was readily interpretable (**Supplementary Fig. 2b–f**). The electron density was weak at the junction where the acyl tail encircled the A′ pocket in the XV19 TCR–CD1d-sulfatide complex, similar to that in the binary CD1d-sulfatide structure, and the final conformation of the acyl tail in the ternary complex was modeled in a counterclockwise direction, similar to the binary structure[28]. Unless stated otherwise, we have compared the XV19 TCR–CD1d-sulfatide complex with the type I $V_\beta8.2$ NKT cell TCR–CD1d–α-GalCer complex[15].

The XV19 TCR docked above the extreme end of the A′ pocket of CD1d (**Fig. 2a**). This structure provided immediate insight into the contrasting nature of the recognition of CD1d-antigen by type I NKT cell TCRs and by the XV19 TCR, as all type I NKT cell TCRs dock over the F′ pocket of CD1d regardless of the chemical nature of the antigen[3,4] (**Fig. 2b**). The contrasting footprints were consistent with different effects of CD1d-specific antibodies and CD1d mutants in their ability to block activation of type I and type II NKT cell lines[28,29]. The disparate recognition modes of type II and type I NKT cell TCRs was reflected in the difference in their centers of gravity above the antigen-binding cleft of CD1d: 25 Å and 37 Å for the V_α and V_β chains, respectively (**Fig. 2c**,**d**). The XV19 TCR docked orthogonally

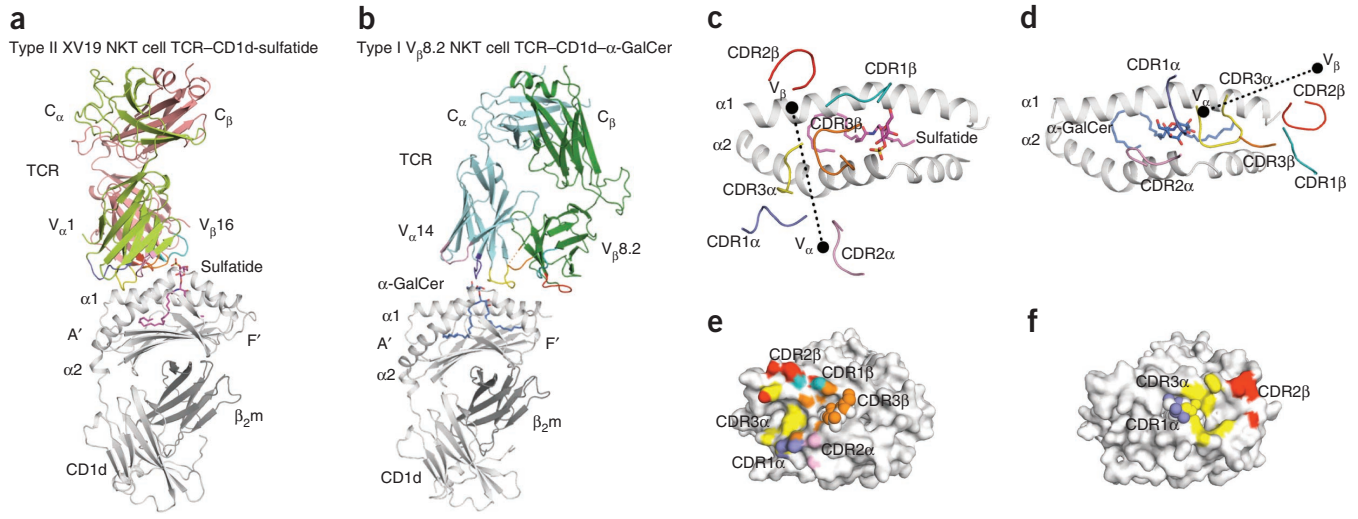

Figure 2 Overview of the docking of the type II NKT cell TCR. (**a**) The XV19 TCR in complex with CD1d-sulfatide: sulfatide, magenta; CD1d heterodimer, gray; V_α1, light green; V_β16, salmon; CDR1α, purple; CDR2α, pink; CDR3α, yellow; CDR1β, teal; CDR2β, red; CDR3β, orange. Only the first 11 carbons of the sulfatide sphingosine tail in the F′ pocket were modeled. (**b**) The type I V_β8.2 NKT cell TCR in complex with CD1d–α-GalCer: α-GalCer, blue; V_α14, cyan; V_β8.2, dark green; colors of CD1d and CDR loops as in **a**. CDR3β (orange dashed lines) is not modeled completely (Protein Data Bank accession code, 3HE6)[15]. (**c**) The XV19 TCR–CD1d-sulfatide complex, viewed down into the cleft of CD1d. Black filled circles indicate the center of mass for the V_α and V_β domains; colors of CD1d and CDR loops as in **a**. (**d**) The type I V_β8.2 NKT cell TCR–CD1d–α-GalCer complex, viewed down into the cleft of CD1d (colors as in **a**,**c**). (**e**) Footprint of the XV19 TCR on the surface of CD1d-sulfatide: sulfatide, gray spheres; colors of CD1d and CDR loops as in **a**. (**f**) Footprint of the type I V_β8.2 NKT cell TCR on the surface of CD1d–α-GalCer: α-GalCer, gray spheres; colors of CD1d and CDR loops as in **a**. Footprint based on atomic contacts.

(100° angle) to the antigen-binding cleft of CD1d, in contrast to the parallel docking mode (20° angle) adopted by type I NKT cell TCRs (**Fig. 2c**,**d**). Furthermore, there were almost no common CD1d-interacting residues in the footprints of the XV19 TCR and V_β8.2 NKT cell TCR (**Fig. 2e**,**f** and **Supplementary Fig. 3**). Collectively, these observations showed how diversity in the type I and type II NKT cell TCR repertoire resulted in very different footprints on CD1d.

XV19 TCR–CD1d interactions

The XV19 TCR was positioned over CD1d such that the α- and β-chains spanned residues 65–72 and 154–167 of the α1 helix and α2 helix of CD1d, respectively, with a buried surface area (BSA) of approximately 1,000 Å^2 after ligation (**Table 1**). The XV19 TCRα and TCRβ chains contributed approximately equivalently to the BSA at the interface, with all CDRs engaging CD1d-sulfatide, albeit to very different extents (**Fig. 2e**). Specifically, the CDR1α, CDR2α and CDR3α loops of the α-chain contributed 5%, 12% and 30% of the BSA, respectively, whereas the CDR1β, CDR2β and CDR3β loops of the β-chain contributed 6%, 7% and 29% of the BSA, respectively. The remaining contributions arose from framework-associated regions that contributed to the BSA of the interaction but did not directly contact CD1d (data not shown). Accordingly, the non-germline-encoded CDR3 loops dominated the interactions at the XV19 TCR–CD1d-sulfatide interface (**Fig. 2e**). These features were in contrast to those of the V_β8.2 NKT cell TCR–CD1d–α-GalCer interaction. In that complex, the V_β8.2 NKT cell TCR interacted with CD1d residues spanning 76–87 and 149–153 of the α1 and α2 helices respectively, and buried 760 Å^2 after ligation. In that type I NKT cell TCR–CD1d-antigen interface, the V_α14-J_α18 chain contributed approximately three times more BSA than did the V_β8.2 chain (**Fig. 2f**). Furthermore, the V_β8.2 NKT cell TCR–CD1d interface was dominated by germline-encoded interactions, whereby the CDR2β loop of the V_β chain exclusively contacted CD1d, whereas the CDR1α loop and CDR3α loop of the J_α18 chain interacted with CD1d–α-GalCer (**Fig. 2f**).

The CDR1α loop of the XV19 TCR was situated peripherally to the α2 helix of CD1d such that only one residue, Tyr32α, interacted with CD1d, with the tip of its aromatic ring nestled between a glycan moiety attached to Asn165, Met162 and Asp166 of CD1d, the latter of which formed a hydrogen bond with Tyr32α (**Fig. 3a**). Tyr32α packed against Phe51α of the CDR2α loop of the XV19 TCR, which contacted Met162 and Ala158 of CD1d, whereas Ser52α formed a hydrogen bond with Gln161 of CD1d. In addition, the CDR2α loop (Ser52α and Asp53α) abutted the same glycosylation site on CD1d as the CDR1α loop did (**Fig. 3a**). The affinity of the XV19 TCR for deglycosylated CD1d-sulfatide suggested that these glycan moieties did not contribute to the affinity of the interaction (data not shown). The CDR1β loop was positioned directly above the α1-helical axis of CD1d, with Leu30β and Tyr31β of the XV19 TCR contacting Val72 and His68 of CD1d, respectively (**Fig. 3b**). Similarly, Tyr50β of the CDR2β loop packed against His68 of CD1d and was the only CDR2β residue that contacted CD1d (**Fig. 3b**). Notably, both V_β8.2 and V_β7 type I NKT cell TCRs have a tyrosine residue at a position in the CDR2β loop equivalent to that of the tyrosine of the XV19 TCR, yet they interact with a completely distinct region of CD1d[15]. Additionally, the CDR2β framework residues Met55β and Glu56β interacted with CD1d. Specifically, Met55β made van der Waals interactions with Glu64 and His68 of CD1d, whereas Glu56β formed a salt bridge to Lys65 of CD1d. Accordingly, whereas the germline-encoded contacts dominate the interaction for type I NKT cell TCRs, the germline-encoded XV19 TCR contacts mediated by V_α and V_β showed a rather tenuous 'finger-grip' hold on CD1d.

In contrast, the CDR3α and CDR3β loops of the XV19 TCR dominated the interactions; the CDR3α loop contacted CD1d only, whereas the CDR3β loop contacted CD1d and the sulfatide antigen. The CDR3α loop was positioned between and contacted both the α1 and α2 helices of CD1d. Tyr97α resided centrally in the CDR3α loop, nestled snugly in a hydrophobic pocket lined by Leu66, Met69 and Leu163 of CD1d, and also formed a hydrogen bond to Thr167 and the main chain of Leu163 of

Table 1 Contacts at the XV19 TCR–CD1d-sulfatide interface

CDR	TCR region	XV19 TCR	CD1d	Bond
CDR1α	V_α	Tyr32$^{O\eta}$	Asp166$^{O\varepsilon1}$, Asp166$^{O\varepsilon2}$	H bond
	V_α	Tyr32	Met162, Asp166	VDW
CDR2α	V_α	Phe51	Met162, Ala158	VDW
	V_α	Ser52$^{O\gamma}$	Gln161$^{N\varepsilon2}$	H bond
CDR3α	N	Gln94	Asp166	VDW
	J_α	Asn95	Asp166, Thr167, Leu170	VDW
	J_α	Asn95$^{O\delta1}$	Thr167$^{O\gamma}$	H bond
	J_α	Asn96	Lys65	VDW
	J_α	Asn96$^{O\delta1}$	Lys65$^{N\zeta}$	H bond
	J_α	Tyr97	Leu66, Thr167, Met162, Leu163	VDW
	J_α	Tyr97$^{O\eta}$	Leu163^{N}, Thr167$^{O\gamma}$	H bond
	J_α	Ala98°	Lys65$^{N\zeta}$	H bond
	J_α	Ala98	Lys65	VDW
CDR1β	V_β	Leu30	Val72	VDW
	V_β	Tyr31	His68	VDW
CDR2β	V_β	Tyr50	His68, Val72	VDW
CDR2β FW	V_β	Met55	Glu64, His68	VDW
	V_β	Glu56$^{O\varepsilon1}$	Lys65$^{N\zeta}$	Salt bridge
	V_β	Glu56$^{O\varepsilon2}$	Lys65$^{N\zeta}$	Salt bridge
CDR3β	D_β	Trp97	Val72, Met69, Gly155	VDW
	J_β	Tyr100	Ala158, Met162	VDW
CDR		XV19 TCR	Sulfatide	Bond
CDR3β	N	Phe96	Sulfate-O8^{H}	VDW
	N	Phe96	C4^{H}, C5^{H}, C6^{H}, 6-OH^{H}	VDW
	D_β	Trp97	C1^{H}, C2^{H}, 2-OH^{H}, sulfate-O10^{H}	VDW
	D_β	Trp97	C^{L}, O^{L}, N^{L}, C18^{L}, O2^{L}, C19^{L}	VDW
	D_β	Trp97$^{N\varepsilon1}$	2-OH^{H}, sulfate-O10^{H}	H bond
	N	Ala101	Sulfate-O10^{H}	VDW

Positions and types of atomic contacts between the TCR and either CD1d or sulfatide, assessed with the CCP4i implementation of CONTACT and a cutoff of 4.5 Å: van der Waals interactions (VDW) are defined as non-hydrogen-bond contact distances of 4 Å or less; hydrogen-bond (H bond) interactions are defined as contact distances of 3.5 Å or less; salt-bridge interactions are defined as contact distances of 4.5 Å or less. Superscripted designations indicate the element involved in hydrogen bonding or salt bridges; superscripted 'H' indicates contacts with the head group; superscripted 'L' indicates contacts with the lipid tail, including the glycosidic linkage. N, nontemplated region of the TCR; FW, framework.

CD1d (**Fig. 3c**). Notably, Leu66, Leu163 and Thr167 are conserved across all human CD1 molecules, which suggests that mouse and human type II NKT cell TCRs and CD1a-, CD1b- and CD1c-restricted TCRs may use these residues for docking (**Supplementary Fig. 3**). Asn95α, which flanked Tyr97α, also formed a hydrogen bond with Thr167, whereas Gln94α was situated more peripherally to the interface and contacted Asp166 of CD1d (**Fig. 3c**). The remaining interactions with the CD1d α1 helix arose principally from hydrogen bonds between Lys65 and Asn96α of the TCR and the main chain of Ala98α. The CDR3β loop, which folded back toward and packed against the CDR3α loop, lay more adjacent to the α2 helix of CD1d. Most notable was the presence of three bulky aromatic residues in this loop (Phe96β, Trp97β and Tyr100β), which were important in contacting CD1d and sulfatide. In this interaction, Trp97β (of β-chain diversity region 2 ($D_\beta2$)) and Tyr100β (of $J_\beta2.1$) acted like two pegs that flanked the α2-helical axis, with Tyr100β packing against Tyr97α and the main chain of CDR3α loop forming van der Waals contacts with Met162 of CD1d (**Fig. 3c**). Thus, the non-germline-encoded CDR3α loop had the major role in contacting CD1d of the XV19 TCR, in contrast to the germline-encoded loops that dominate contacts of type I NKT cell TCRs with CD1d-antigen.

TCR plasticity and sulfatide interactions

Having determined the structure of the unligated XV19 TCR, we addressed the extent of conformational change after formation of the XV19 TCR–CD1d-sulfatide complex. Furthermore, as the binary structure of CD1d-sulfatide was available[27], we evaluated the degree of plasticity in CD1d and the sulfatide antigen after engagement by the XV19 TCR. In comparing the structure of CD1d-sulfatide in the ligand-bound and binary state, we found essentially no movement in CD1d itself (r.m.s. deviation of 0.47 Å), with Glu64, His68, Met69, Met162 and Leu170 representing the side chains that changed conformation after formation of the complex (data not shown). The conformation of the hydrophobic roof (Leu84, Val149 and Leu150) above the F′ pocket[6] seemed unchanged after ligation. In the ternary complex, the sulfatide head group leaned toward the α2 helix of CD1d, protruding upright from the antigen-binding cleft (**Fig. 4a**). The sulfated head group showed limited movement after ligation of the XV19 TCR (**Fig. 4b**). In contrast, when type I NKT cell TCRs bind to β-linked ligands[8], the glycosyl head groups are flattened to resemble the conformation of the α-linked counterparts. In the XV19 TCR–CD1d-sulfatide complex, the sulfatide antigen was contacted solely by the CDR3β loop (**Fig. 4a**). Phe96β and Trp97β of the CDR3β loop sequestered one side

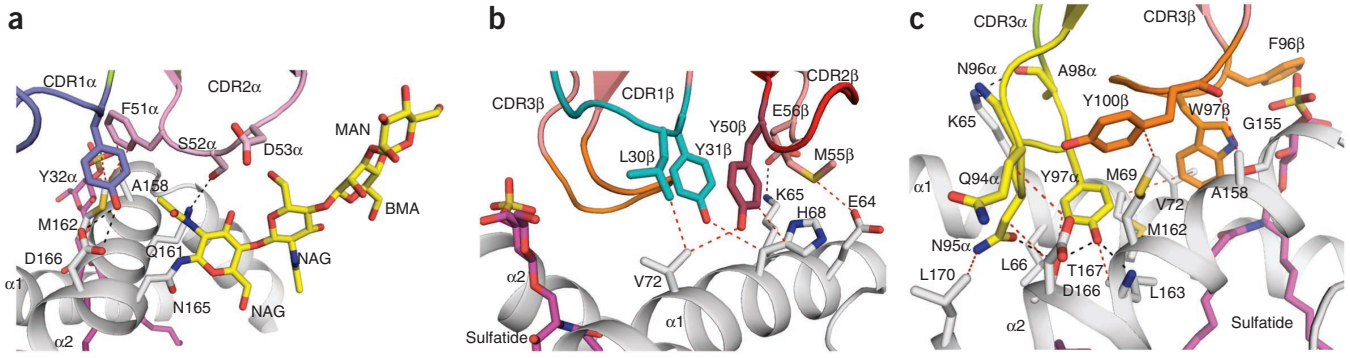

Figure 3 Contacts between the XV19 TCR and CD1d. (**a**) Contacts between CDR1α (purple) and CDR2α (pink) of the XV19 TCR and CD1d; yellow indicates glycosylation sites (N-acetylglucosamine (NAG), β-mannose (BMA) and α-mannose (MAN)). (**b**) Contacts between CDR1β (teal) and CDR2β (red) of the XV19 TCR and CD1d. CDR3β, orange. (**c**) Contacts between CDR3α (yellow) and CDR3β (orange) of the XV19 TCR and CD1d (gray): sulfatide, magenta; hydrogen-bond interactions, black dashed lines; van der Waals interactions, red dashed lines.

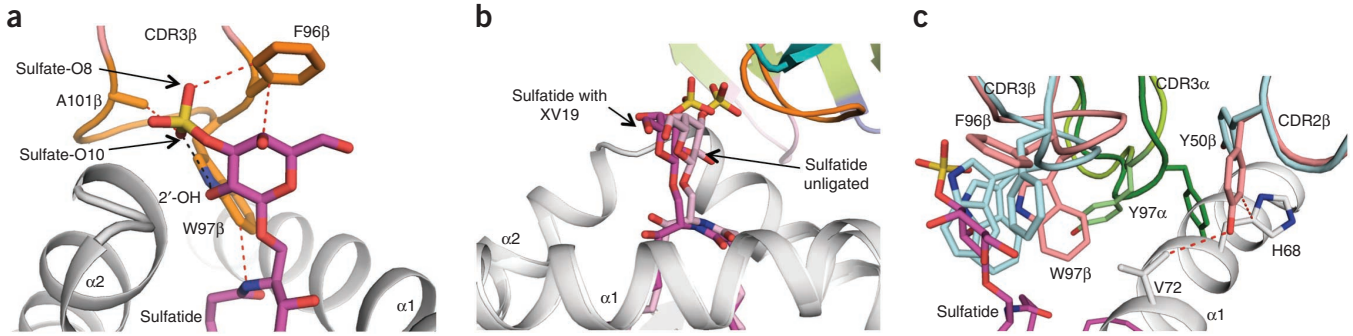

Figure 4 Sulfatide-mediated contacts between the XV19 TCR and CD1d. (**a**) Contacts between CDR3β (orange) of the XV19 TCR and sulfatide (magenta). CD1d, gray; van der Waals interactions shown in red dashed lines. (**b**) Conformation of sulfatide in CD1d-sulfatide (Protein Data Bank accession code, 2AKR)[27] and XV19 TCR–CD1d-sulfatide. CD1d, gray; sulfatide, magenta in XV19 TCR–CD1d-sulfatide or pink in CD1d-sulfatide. The sugar head group is standing upright. (**c**) Overlay of the XV19 TCR (V_α, dark green; V_β, cyan) onto XV19 TCR–CD1d-sulfatide (V_α, light green; V_β, salmon); sulfatide, magenta; CD1d, gray.

of the glycosyl head group, with the sulfate moiety wedged between the α2 helix and Phe96β, and formed a hydrogen bond with Trp97β, the latter of which also formed a hydrogen bond with the 2-OH group of the glycosyl moiety (**Fig. 4a**). Collectively, the sulfatide antigen contributed 7% of the BSA of the interaction with the XV19 TCR. Although the conformation of the sulfated moiety was stabilized in a well-defined pocket, it nevertheless did not form an intricate hydrogen-bonding network, which suggested that unsulfated β-linked lipids could also act as antigens for this type II NKT cell TCR, consistent with reports showing that the XV19 TCR can be stimulated, albeit to a lesser extent, with β-GlcCer[30].

Although the XV19 TCR showed limited plasticity in engaging CD1d-sulfatide, there was nevertheless some reorientation of side-chain and main-chain conformations after ligation. Most notably, Tyr97α swiveled approximately 9 Å to avoid steric clashes with CD1d, which subsequently resulted in remodeling of the conformation of the CDR3α loop (**Fig. 4c**). Similarly, Tyr50β of the CDR2β loop flipped its conformation to avoid clashing with CD1d and subsequently contacted His68 and Val72 of CD1d (**Fig. 4c**). Furthermore, the aromatic rings of Phe96β and Trp97β were repositioned by approximately 4 Å to avoid steric clashes with the sulfatide antigen, which also resulted in a remodeling of the main chain (residues 96–98) of the CDR3β loop (**Fig. 4c**). However, Tyr50b and CDR3b were involved in crystal contacts in the unligated XV19 TCR crystal lattice. Regardless, we found that in contrast to recognition by type I NKT cell TCRs, in which the germline-encoded loops force conformational changes after ligation of the CD1d-antigen, recognition by the XV19 TCR was characterized by the molding of hypervariable CDR loops around CD1d-sulfatide.

Energetics of the type II NKT cell TCR–CD1d-antigen interaction

Given that the CDR3 loops of the XV19 TCR dominated the structural contacts with CD1d-sulfatide, we next established whether these loops were energetically important for the XV19 TCR–CD1d-sulfatide interaction. On the basis of the XV19 TCR-CD1d-sulfatide

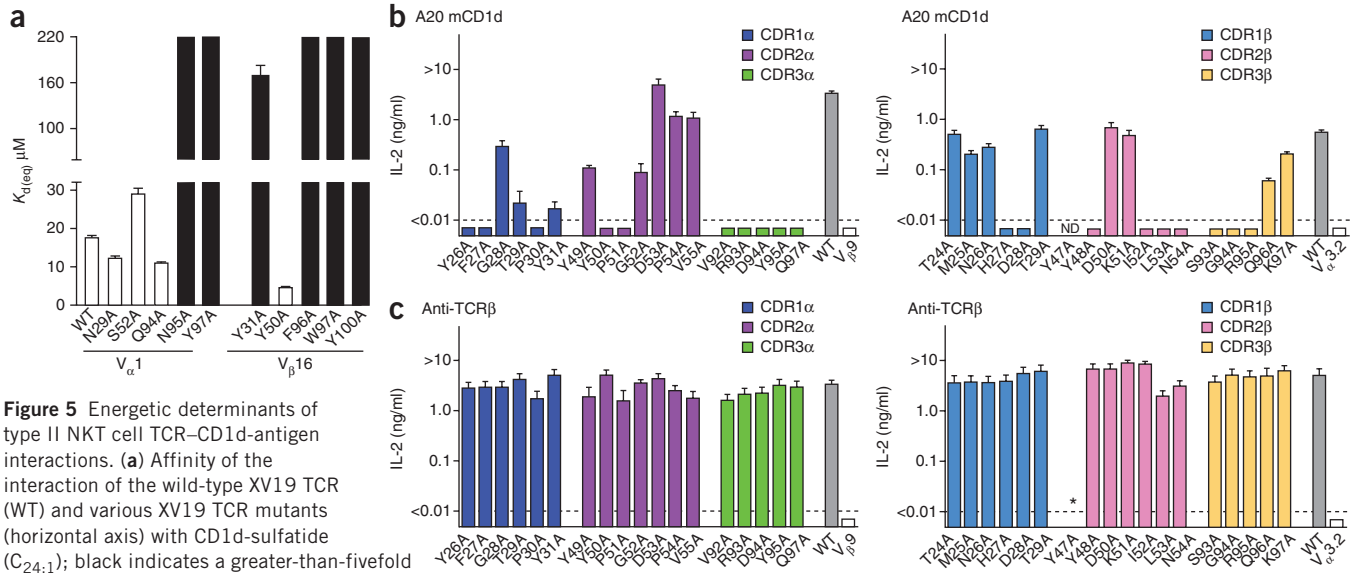

Figure 5 Energetic determinants of type II NKT cell TCR–CD1d-antigen interactions. (**a**) Affinity of the interaction of the wild-type XV19 TCR (WT) and various XV19 TCR mutants (horizontal axis) with CD1d-sulfatide ($C_{24:1}$); black indicates a greater-than-fivefold effect. Results are presented as the equilibrium dissociation constant ($K_{d(eq)}$). (**b**,**c**) Enzyme-linked immunosorbent assay of IL-2 production by hybridomas expressing wild-type or mutant α-chains (left) and β-chains (right) of the VIII24 type II NKT cell TCR (V_α3.2-V_β9), stimulated overnight with A20 cells transfected to express mouse CD1d in the absence of exogenous antigen (A20 mCD1d; **b**) or plate-bound monoclonal antibody to TCRβ (2.5 μg/ml; Anti-TCRβ; **c**). V_β9 or V_α3.2 (far right), hybridomas infected to express TCRβ or TCRα only and sorted on the basis of expression of the reporter gene. ND, not determined (the βY47A substitution resulted in little to no TCR expression and therefore could not be studied). Data are from two (mutant TCRs) or eight (wild-type TCR) separate experiments (**a**; mean and s.e.m.) or represent three (**b**,**c**; TCRα mutants) or two (**b**,**c**; TCRβ mutants) independent experiments with triplicate cultures (**b**,**c**; mean and s.e.m.).

structure, we targeted ten XV19 TCR residues for substitution with alanine (five each from the TCRα and TCRβ chains). We replaced Gln94α, Asn95α and Tyr97α of the CDR3α loop and Phe96β, Trp97β and Tyr100β of the CDR3β loop. We also replaced Ser52α of the CDR2α loop, Tyr31β of the CDR1β loop and Tyr50β of the CDR2β loop to assess the role of the germline-encoded residues in the XV19 TCR–CD1d-sulfatide interaction. As a control, we also replaced Asn29α, a residue not involved in the XV19 TCR–CD1d-sulfatide interaction. The mutant XV19 TCRs were expressed and refolded with yields similar to that of wild-type XV19 TCR and had chromatographic properties similar to those of the wild-type XV19 TCR; the wild-type and mutant XV19 TCRs also had similar properties by SDS-PAGE under reducing and nonreducing conditions (data not shown). We assessed by surface plasmon resonance the effect of those substitutions on the affinity of the XV19 TCR–CD1d-sulfatide interaction (**Fig. 5a** and **Supplementary Figs. 4** and **5**) and categorized them as having no effect, a moderate effect (three- to fivefold loss of affinity) or a 'marked' effect (loss of affinity of more than fivefold). As expected, the N29αA control substitution did not affect the affinity of the interaction, and neither did the S52αA substitution, whereas the Y50βA mutant moderately improved the affinity of the interaction. The Q94αA mutant from the CDR3α loop also did not affect the affinity, which was expected, as Gln94α was situated at the periphery of the interface (**Fig. 3c**). In contrast, substitution Tyr31β, Asn95α, Tyr 97α, Phe96β, Trp97β or Tyr100β each had a considerable effect on the affinity of the interaction. Tyr31β barely contacted CD1d-sulfatide, and we attribute the substantial effect of the Y31βA mutant to destabilization of the local conformation of the XV19 TCR, as the aromatic ring of Tyr31β packed closely against the CDR2β and CDR3β loops. Collectively, the XV19 mutagenesis data were consistent with the structural data and supported the finding of involvement of the CDR3α loop and CDR3β loop in the interaction with CD1d and the sulfatide antigen, respectively.

Next we undertook mutagenesis studies to determine the relative roles the CDR loops of a different type II NKT cell TCR, the autoreactive VIII24 NKT cell TCR[21]. This TCR is composed of V_α3.2-J_α26–V_β9-J_β1-4 and thus is distinct from the XV19 TCR (V_α1-J_α26–V_β16-J_β2.1). We transfected the 5KC-78.3.20 mouse T cell hybridoma to express the wild-type VIII24 TCR or each of 35 different single-site mutants of the VIII24 TCR. We confirmed equivalent cell-surface expression by expression of a reporter gene as well as by staining with antibody to TCRβ. We assessed the ability of the transfectants to be activated by endogenous CD1d transfected into the A20 mouse B cell lymphoma line or by plate-bound antibody to TCRβ (**Fig. 5b**,**c**). The data indicated that some residues of the CDR1 and CDR2 loops were important for the interaction but also that the non-germline-encoded CDR3α and CDR3β loops had a critical role in the binding of the VIII24 TCR to CD1d-antigen. Although the effects of some of these mutants were potentially indirect, the data supported the hypothesis that type II NKT cell TCRs may vary in their CD1d-antigen contacts but also that non-germline-encoded CDR3α and CDR3β loops of type II NKT cell TCRs can have a key role in the recognition of CD1d-antigen.

DISCUSSION

Type II NKT cells are considered to be functionally distinct from type I NKT cells[21,31]. However, the understanding of the function of type II NKT cells in the immune system, the antigens they respond to and why their CD1d-restricted antigen specificity is different from that of type I NKT cells remains unclear. Central to the understanding of type II NKT cell biology is elucidating how their TCRs recognize CD1d-restricted antigens.

A series of studies have provided insight into the molecular basis of the recognition of CD1d-antigen by type I NKT cell TCRs[5,6,8,9,11,14–16,25,32–37]. The type I NKT cell TCR acts like a relatively rigid pattern-recognition receptor regardless of the nature of the type I antigen. The type I NKT cell TCR–CD1d interaction is dominated by interactions with germline-encoded regions of the invariant V_α-J_α chain and the V_β chain. These features define the recognition of-CD1d-antigen by type I NKT cell TCRs and, given that the canonical features of this footprint are maintained in the V_α10-J_α50 NKT cell TCR–CD1d–α-GlcCer complex[33], it has remained unclear how type II NKT cell TCRs engage CD1d-antigen.

Notably, the ternary structure of a type II NKT cell TCR–CD1d-antigen complex has shown that the mode of interactions for a type I and type II NKT cell TCR can be very different, not only in terms of the footprint on CD1d but also in the relative characteristics at the interface. The XV19 TCR docked orthogonally above the A′ pocket of CD1d-sulfatide, and the interactions of germline-encoded regions were suboptimal for CD1d engagement. Instead, the non-germline-encoded loops of the XV19 TCR dominated the interface, with the CDR3α loop making multiple contacts with CD1d and the CDR3β loop determining the specificity for the sulfatide antigen. Moreover, the CDR3 loops showed a moderate degree of flexibility in engaging CD1d-sulfatide, whereas the sulfatide head group remained fixed after engagement of the XV19 TCR. The results of the associated mutagenesis studies supported the structural data, showing that the CDR3α and CDR3β loops underpinned the energetics of the XV19 TCR–CD1d-sulfatide interaction. Thus, for the XV19 TCR, it seemed that the CDR3α loop was selected for reactivity with CD1d, whereas the CDR3β loop was selected for antigen specificity. Notably, the mutagenesis data for the VIII24 type II NKT cell TCR also showed that the non-germline-encoded CDR3 loops had a key role in mediating autoreactivity to CD1d and, furthermore, CDR1 and CDR2 loops also contributed to this interaction. Collectively, these features of the interactions of the XV19 and VIII24 type II NKT cell TCRs with CD1d-antigen were reminiscent of the recognition of TCR–peptide–major histocompatibility complex, in which the non-germline-encoded loops often have a role in directly determining antigen specificity[26,38,39]. Moreover, the extreme A′ pocket focus of the XV19 TCR resonated with the extreme amino-terminal footprint that some TCRs can adopt on peptide–major histocompatibility complex[40,41].

Varied use of V_α-V_β TCRs can 'translate' into differing docking modes and altered fine specificity for the peptide antigen after ligation to a common HLA molecule[42]. Our findings have provided a description of how altered TCR use resulted in a differing docking solution on a monomorphic antigen-presenting molecule. At the population level, type II NKT cells can show biased V_α-V_β use, although they have greater TCR diversity than that of type I NKT cells[19–21]. This observation raises the possibility that there are many different docking solutions underpinning type II NKT cell TCR–CD1d-antigen interactions that are governed by the antigen and the responding NKT cell repertoire. That idea is supported by the finding of distinct energetically important regions of the VIII24 and XV19 type II NKT cell TCRs. It is also consistent with the ability of type II NKT cells to respond to a wide range of antigens, including sulfatides, phospholipids, other glycolipids and nonlipidic antigens[43–45]. Notably, conserved use of CDR3β has been observed, at least in the sulfatide-reactive fraction of type II NKT cell TCRs[20]. Given the principal role of the CDR3β loop in determining antigen specificity for the XV19 TCR–CD1d-sulfatide interaction, conserved CDR3β use might reflect common interactions for type II NKT cells with sulfatide and possibly other antigens for

type II NKT cell. We speculate that type II NKT cells may be better suited to bind β-linked self glycolipids, such as sulfatide, rather than microbe-based α-linked glycolipid antigens.

Collectively, the crystal structure and associated mutagenesis data presented here for a type II NKT cell TCR–CD1d-antigen complex have provided a foundation for understanding the fundamental basis of type II NKT cell reactivity. Although it is known that TCRs of the type I NKT cell repertoire exclusively contact the F′ pocket of CD1d, we have now shown that the immune system has a mechanism for interacting with a completely distinct region of CD1d. This finding provides a basis for understanding the diverse specificity of lipid antigen-reactive T cells and demonstrates that the TCR will gain a foothold onto any feature of an antigen-presenting molecule that lends itself for immunosurveillance[46].

METHODS

Methods and any associated references are available in the online version of the paper.

Accession codes. Protein Data Bank: XV19 TCR, 4EI6; XV19 TCR–CD1d-sulfatide ($C_{24:1}$) complex, 4EI5.

Note: Supplementary information is available in the online version of the paper.

ACKNOWLEDGMENTS

We thank the staff at the MX2 beamline of the Australian synchrotron for assistance with data collection and Monash Macromolecular Crystallisation Facility for crystallization experiments. Supported by the National Health and Medical Research Council of Australia (D.I.G. and J.R.), the Australian Research Council, the Cancer Council of Victoria, the US National Institutes of Health (AI090450 and AI092108 to L.G.), the Swedish Research Council (S.L.C.), the Swedish Cancer Society (S.L.C.) and Monash University (S.G. and J.R.).

AUTHOR CONTRIBUTIONS

O.P., D.G.P. and S.G. generated and analyzed data; M.L.S.-R., A.J.C., A.T., A.P.U., J.L.N., T.M. and L.G. generated data; S.L.C. provided the XV19 and VIII24 cells; and D.I.G. and J.R. together led the investigation, devised the project, analyzed the data and wrote the manuscript.

COMPETING FINANCIAL INTERESTS

The authors declare no competing financial interests.

Published online at http://www.nature.com/doifinder/10.1038/ni.2372.
Reprints and permissions information is available online at http://www.nature.com/reprints/index.html.

1. Godfrey, D.I., MacDonald, H.R., Kronenberg, M., Smyth, M.J. & Van Kaer, L. NKT cells: what's in a name? *Nat. Rev. Immunol.* **4**, 231–237 (2004).
2. Terabe, M. & Berzofsky, J.A. NKT cells in immunoregulation of tumor immunity: a new immunoregulatory axis. *Trends Immunol.* **28**, 491–496 (2007).
3. Joyce, S., Girardi, E. & Zajonc, D.M. NKT cell ligand recognition logic: molecular basis for a synaptic duet and transmission of inflammatory effectors. *J. Immunol.* **187**, 1081–1089 (2011).
4. Godfrey, D.I. *et al.* Antigen recognition by CD1d-restricted NKT T cell receptors. *Semin. Immunol.* **22**, 61–67 (2010).
5. Borg, N.A. *et al.* CD1d-lipid-antigen recognition by the semi-invariant NKT T-cell receptor. *Nature* **448**, 44–49 (2007).
6. Li, Y. *et al.* The Va14 invariant natural killer T cell TCR forces microbial glycolipids and CD1d into a conserved binding mode. *J. Exp. Med.* **207**, 2383–2393 (2010).
7. López-Sagaseta, J., Sibener, L.V., Kung, J.E., Gumperz, J. & Adams, E.J. Lysophospholipid presentation by CD1d and recognition by a human natural killer T-cell receptor. *EMBO J.* **31**, 2047–2059 (2012).
8. Pellicci, D.G. *et al.* Recognition of β-linked self glycolipids mediated by natural killer T cell antigen receptors. *Nat. Immunol.* **12**, 827–833 (2011).
9. Yu, E.D., Girardi, E., Wang, J. & Zajonc, D.M. Cutting edge: structural basis for the recognition of β-linked glycolipid antigens by invariant NKT cells. *J. Immunol.* **187**, 2079–2083 (2011).
10. Scott-Browne, J.P. *et al.* Germline-encoded recognition of diverse glycolipids by natural killer T cells. *Nat. Immunol.* **8**, 1105–1113 (2007).
11. Mallevaey, T. *et al.* A molecular basis for NKT cell recognition of CD1d-self-antigen. *Immunity* **34**, 315–326 (2011).
12. Mallevaey, T. *et al.* T cell receptor CDR2β and CDR3β loops collaborate functionally to shape the iNKT cell repertoire. *Immunity* **31**, 60–71 (2009).
13. Matulis, G. *et al.* Innate-like control of human iNKT cell autoreactivity via the hypervariable CDR3β loop. *PLoS Biol.* **8**, e1000402 (2010).
14. Patel, O. *et al.* Vb2 natural killer T cell antigen receptor-mediated recognition of CD1d-glycolipid antigen. *Proc. Natl. Acad. Sci. USA* **108**, 19007–19012 (2011).
15. Pellicci, D.G. *et al.* Differential recognition of CD1d-α-galactosyl ceramide by the Vβ8.2 and Vβ7 semi-invariant NKT T cell receptors. *Immunity* **31**, 47–59 (2009).
16. Adams, E.J. & Lopez-Sagaseta, J. The immutable recognition of CD1d. *Immunity* **34**, 281–283 (2011).
17. Blomqvist, M. *et al.* Multiple tissue-specific isoforms of sulfatide activate CD1d-restricted type II NKT cells. *Eur. J. Immunol.* **39**, 1726–1735 (2009).
18. Jahng, A. *et al.* Prevention of autoimmunity by targeting a distinct, noninvariant CD1d-reactive T cell population reactive to sulfatide. *J. Exp. Med.* **199**, 947–957 (2004).
19. Park, S.H. *et al.* The mouse CD1d-restricted repertoire is dominated by a few autoreactive T cell receptor families. *J. Exp. Med.* **193**, 893–904 (2001).
20. Arrenberg, P., Halder, R., Dai, Y., Maricic, I. & Kumar, V. Oligoclonality and innate-like features in the TCR repertoire of type II NKT cells reactive to a β-linked self-glycolipid. *Proc. Natl. Acad. Sci. USA* **107**, 10984–10989 (2010).
21. Cardell, S. *et al.* CD1-restricted CD4$^+$ T cells in major histocompatibility complex class II-deficient mice. *J. Exp. Med.* **182**, 993–1004 (1995).
22. Bai, L. *et al.* Lysosomal recycling terminates CD1d-mediated presentation of short and polyunsaturated variants of the NKT cell lipid antigen αGalCer. *Proc. Natl. Acad. Sci. USA* **106**, 10254–10259 (2009).
23. Im, J.S. *et al.* Kinetics and cellular site of glycolipid loading control the outcome of natural killer T cell activation. *Immunity* **30**, 888–898 (2009).
24. Sullivan, B.A. *et al.* Mechanisms for glycolipid antigen-driven cytokine polarization by Vα14i NKT cells. *J. Immunol.* **184**, 141–153 (2010).
25. Wun, K.S. *et al.* A molecular basis for the exquisite CD1d-restricted antigen specificity and functional responses of natural killer T cells. *Immunity* **34**, 327–339 (2011).
26. Godfrey, D.I., Rossjohn, J. & McCluskey, J. The fidelity, occasional promiscuity, and versatility of T cell receptor recognition. *Immunity* **28**, 304–314 (2008).
27. Zajonc, D.M. *et al.* Structural basis for CD1d presentation of a sulfatide derived from myelin and its implications for autoimmunity. *J. Exp. Med.* **202**, 1517–1526 (2005).
28. Monzon-Casanova, E. *et al.* CD1d expression in Paneth cells and rat exocrine pancreas revealed by novel monoclonal antibodies which differentially affect NKT cell activation. *PLoS ONE* **5**, e13089 (2010).
29. Burdin, N. *et al.* Structural requirements for antigen presentation by mouse CD1. *Proc. Natl. Acad. Sci. USA* **97**, 10156–10161 (2000).
30. Brennan, P.J. *et al.* Invariant natural killer T cells recognize lipid self antigen induced by microbial danger signals. *Nat. Immunol.* **12**, 1202–1211 (2011).
31. Exley, M.A. *et al.* Cutting edge: A major fraction of human bone marrow lymphocytes are Th2-like CD1d-reactive T cells that can suppress mixed lymphocyte responses. *J. Immunol.* **167**, 5531–5534 (2001).
32. Patel, O. *et al.* NKT TCR recognition of CD1d-α-C-galactosylceramide. *J. Immunol.* **187**, 4705–4713 (2011).
33. Uldrich, A.P. *et al.* A semi-invariant $V_\alpha 10^+$ T cell antigen receptor defines a population of natural killer T cells with distinct glycolipid antigen-recognition properties. *Nat. Immunol.* **12**, 616–623 (2011).
34. Aspeslagh, S. *et al.* Galactose-modified iNKT cell agonists stabilized by an induced fit of CD1d prevent tumour metastasis. *EMBO J.* **30**, 2294–2305 (2011).
35. Girardi, E. *et al.* Unique interplay between sugar and lipid in determining the antigenic potency of bacterial antigens for NKT cells. *PLoS Biol.* **9**, e1001189 (2011).
36. Wang, J. *et al.* Lipid binding orientation within CD1d affects recognition of *Borrelia burgorferi* antigens by NKT cells. *Proc. Natl. Acad. Sci. USA* **107**, 1535–1540 (2010).
37. Wun, K.S. *et al.* A minimal binding footprint on CD1d-glycolipid is a basis for selection of the unique human NKT TCR. *J. Exp. Med.* **205**, 939–949 (2008).
38. Borg, N.A. *et al.* The CDR3 regions of an immunodominant T cell receptor dictate the 'energetic landscape' of peptide-MHC recognition. *Nat. Immunol.* **6**, 171–180 (2005).
39. Garcia, K.C. *et al.* Structural basis of plasticity in T cell receptor recognition of a self peptide-MHC antigen. *Science* **279**, 1166–1172 (1998).
40. Hahn, M., Nicholson, M.J., Pyrdol, J. & Wucherpfennig, K.W. Unconventional topology of self peptide-major histocompatibility complex binding by a human autoimmune T cell receptor. *Nat. Immunol.* **6**, 490–496 (2005).
41. Gras, S. *et al.* The shaping of T cell receptor recognition by self-tolerance. *Immunity* **30**, 193–203 (2009).
42. Gras, S. *et al.* A structural basis for varied αβ TCR usage against an immunodominant EBV antigen restricted to a HLA-B8 molecule. *J. Immunol.* **188**, 311–321 (2012).
43. Chang, D.H. *et al.* Inflammation associated lysophospholipids as ligands for CD1d restricted T cells in human cancer. *Blood* **112**, 1308–1316 (2008).
44. Dieudé, M. *et al.* Cardiolipin binds to CD1d and stimulates CD1d-restricted γδ T cells in the normal murine repertoire. *J. Immunol.* **186**, 4771–4781 (2011).
45. Van Rhijn, I. *et al.* CD1d-restricted T cell activation by nonlipidic small molecules. *Proc. Natl. Acad. Sci. USA* **101**, 13578–13583 (2004).
46. Tikhonova, A.N. *et al.* αβ T cell receptors that do not undergo major histocompatibility complex-specific thymic selection possess antibody-like recognition specificities. *Immunity* **36**, 79–91 (2012).

ONLINE METHODS

Reagents. Lipids were from Avanti Polar Lipids.

Determination of α- and β-chain sequences of TCRs from T cell hybridomas. The mRNA of the original XV19 T cell hybridoma[21] was extracted with Trizol (Invitrogen) and was reverse-transcribed into cDNA with a cDNA synthesis kit (Superscript III) according to manufacturer's instructions (Invitrogen). The sense oligonucleotides specific for 23 V_β chains and 19 V_α chains and the antisense oligonucleotides for the α-chain and β-chain constant regions have been described[47–49]. PCR conditions were as follows: 35 cycles of 94 °C for 30 s, 60 °C for 45 s and 72 °C for 90 s. PCR products were separated by electrophoresis through a 2% agarose gel and were analyzed by staining with ethidium bromide. Amplified α-chains and β-chains were cloned with TOPO TA cloning kit (Invitrogen) and sequenced. In-frame rearrangements were found for V_α1-J_α26 (TRAV7D-4*02–TRAJ26*01) with the CDR3α sequence of CAASEQNNYAQGLTF and for V_β16-D_β2-J_β2.1 (TRBV3-TRBD2-TRBJ2.1) with the CDR3β sequence of CASSFWGAYAEQFF.

Protein production and purification. Mouse CD1d was produced as described[14]. Sequence encoding recombinant CD1d–β_2-microglobulin with a BirA tag followed by a six-histidine tag was cloned into the pFasBacDual vector (Invitrogen) and was produced in the High Five insect cell line (Invitrogen). Soluble CD1d protein was purified by nickel-agarose affinity purification followed by size exclusion through a Superdex 200 16/60 gel-filtration column. The genes encoding XV19 TCR V_α1 (TRAV7D-4*02-TRAJ26*01) and V_β16 (TRBV3-TRBD2-TRBJ2.1), after codon optimization, were synthesized (Genscript) as chimeric mouse variable-domain–human constant-domain segments and were cloned into the expression vector pET30 (Novogen). The human constant domains included Avidex cysteine residues to aid in refolding as described[15]. XV19 TCR V_α1 and V_β16 were expressed in *Escherichia coli* strain BL21 and were produced in inclusion bodies. Inclusion bodies were resuspended in 8 M urea, 20 mM Tris-HCl, pH 8.0, 0.5 mM Na-EDTA and 1 mM DTT. The XV19 TCR was refolded by dilution in a solution containing 5 M urea, 0.1 M Tris-HCl, pH 8.0, 2 mM Na-EDTA, 400 mM L-arginine-HCl, 0.5 mM oxidized glutathione and 5 mM reduced glutathione. The refolding solution was then dialyzed for elimination of urea. The TCR was purified by DEAE anion exchange, gel filtration and HiTrap-Q anion-exchange chromatography. The functional integrity of the refolded TCR was assessed by reactivity with TCR-specific conformation-dependent monoclonal antibody 12H8 (prepared in-house)[38].

Loading of CD1d with lipid. Lipids were loaded onto CD1d as described[15] by incubation of CD1d overnight at 20 °C with a three to six molar excess of sulfatide. CD1d-sulfatide complexes were isolated by purification with ion-exchange chromatography (Mono Q column, 10/100 GL; GE Healthcare) for separation of sulfatide-loaded CD1d from the endogenous CD1d.

Surface plasmon resonance measurements and analysis. All these experiments were done at 25 °C on a Biacore 3000 with HBS buffer (10 mM HEPES-HCl, pH 7.4, and 150 mM NaCl). For analysis of the reactivity of the XV19 TCR to CD1d-sulfatide, CD1d–α-GalCer and CD1d purified from insect cells with endogenous lipid, lipid-loaded CD1d (~3,000 RU) was bound to a research-grade SA chip and the XV19 TCR (150 μM) was applied at a flow rate of 5 μl/min. This experiment showed some degree of autoreactivity of XV19 TCR to CD1d purified from insect cells with endogenous lipid, and there was a negative response of XV19TCR to CD1d–α-GalCer (**Fig. 1a**, right), as the response was subtracted from that of endogenous CD1d. In subsequent experiments (**Fig. 1b**,**c**), CD1d was loaded with sulfatide and loaded CD1d-sulfatide was separated from endogenous CD1d by ion-exchange chromatography. In these experiments, CD1d loaded with sulfatide was coupled at ~1,300 RU and the equilibrium affinity of the XV19 TCR (0–200 μM) was measured at a flow rate of 30 μl/min. For experiments to determine the equilibrium affinity of the binding of the XV19 TCR mutants, CD1d sulfatide $C_{24:1}$ was bound on the chip at 3,200–3,500 RU. For analysis of the XV19 mutants, each mutant was applied at a flow rate of 5 μl/min (two to three mutants per experiment, with wild-type XV19 TCR included as a control for each). Each mutant was applied at a concentration ranging from 220–0 μM, except N29αA, which was applied at a concentration range of 210–0 μM. The final response was calculated by subtraction of the response of the streptavidin-coated chip alone from that of XV19 TCR–CD1d-sulfatide interaction. BIAevaluation Version 3.1 (Biacore AB) was used to fit the data to the 1:1 Langmuir binding model. GraphPad Prism Version 5.0d was used for data presentation.

Crystallization, structure determination and refinement. The XV19 TCR (6–10 mg/ml in 10 mM Tris-HCl pH8.0, and 150 mM NaCl) was crystallized at room temperature in a solution of 25% PEG 3350 and 0.1 M MIB buffer (sodium malonate, imidazole and boric acid at a molar ratio of 2:3:3) at a pH of 6. The XV19 TCR was mixed with CD1d-sulfatide ($C_{24:1}$), and the ternary complex was isolated by gel filtration on a Superdex 200 16/60 column (GE Healthcare). The XV19 TCR–CD1d-sulfatide complex (6 mg/ml in 10 mM Tris-HCl pH 8.0, and 150 mM NaCl) was crystallized at 20 °C in 12–20% PEG 3350 and 0.1 M citrate–bis-Tris–propane buffer at a pH of 7.1. An equal ratio of the protein to crystallization solution resulted in crystals after 1–2 d. The crystals were flash-frozen before data collection with increasing concentrations of PEG as a cryoprotectant. Crystals of the complex and the XV19 TCR were diffracted to 3.1 Å and 1.7 Å, respectively, at the Australian Synchrotron MX2 facility in Melbourne, Australia. Data for the ternary complex were processed with XDS software and were scaled with the Scala scaling and data-merging program of the CCP4 suite (Collaborative Computational Project number 4)[50]. Crystals of the complex belonged to the space group $P2_12_12_1$ with two ternary complexes in the asymmetric unit. Data for the XV19 TCR were processed with the diffraction data-integration program MOSLFM (version 7.0.5) and were scaled with Scala of the CCP4 Suite[51]. Crystals of the XV19 TCR belonged to the space group $P2_12_12_1$ with two molecules in the asymmetric unit. The crystal structure of the XV19 TCR was solved through the use of a TCR (Protein Data Bank accession code 2BNU) without the CDR loops, and that of the ternary complex was solved through the use of the XV19 TCR and mouse CD1d–sulfatide (Protein Data Bank accession code, 2AKR) without the lipid as a search model by the molecular-replacement method with the PHASER program (for phasing macromolecular crystal structures by maximum-likelihood methods) from the CCP4 Suite. The REFMAC macromolecular refinement program (version 5.5.0109), the Phenix software suite for the automated determination of macromolecular structures (Python-based hierarchical environment for integrated Xtallography; version 1.6.4) and the BUSTER refinement program (version 2.10)[52] were used for refinement, and the COOT program for macromolecular model building, completion and confirmation (Crystallographic Object-Oriented Toolkit) was used for model building. The quality of all structures was confirmed at the website of the Research Collaboratory for Structural Bioinformatics Protein Data Bank Data Validation and Deposition Services. All structural diagrams were created with the PyMOL molecular visualization system[53]. Surface area values were calculated with Areaimol of the CCP4 suite. In the structure of XV19 TCR–CD1d-sulfatide ($C_{24:1}$), only the first 11 carbons of the sulfatide sphingosine tail were modeled, and occupancy of carbons 26–28 in the acyl tail was set at 0.5 because of weak electron density in one molecule of the complex, whereas in the other molecule of the complex, only the first seven carbons of each tail were modeled in the final structure.

VIII24 TCR mutagenesis studies. Wild-type VIII24 TCR was cloned from the original VIII24 hybridoma[21]. Wild-type and mutant chains were generated as described[12]. TCRα and TCRβ chains were generated by PCR with overlapping primers and were inserted into mouse stem cell virus–based plasmids with an internal ribosome entry site plus sequence encoding green fluorescent protein (TCRα) or human nerve growth factor receptor (TCRβ) as the reporter. Retroviruses were produced by transfection into Phoenix producer cell lines, and retrovirus-containing supernatants were used for infection of the 5KC-78.3.20 mouse T cell hybridoma. Cells were sorted on the basis of reporter gene expression and for similar TCR expression. The Y47βA substitution resulted in little to no TCR expression in several independent experiments and therefore was not studied. For stimulation assays, 5×10^4 hybridoma cells were cultured for 20 h with 5×10^4 A20 cells transfected to express mouse CD1d or were cultured for 20 h with plate-bound antibody to TCRβ (2.5 μg/ml; plates precoated for 2 h with antibody in 50 μl PBS; H57-597; eBioscience) in complete RPMI medium containing

doi:10.1038/ni.2372

10% (vol/vol) FCS. Hybridoma responses were measured by enzyme-linked immunosorbent assay of IL-2 according to standard protocols.

47. Cochet, M. *et al*. Molecular detection and *in vivo* analysis of the specific T cell response to a protein antigen. *Eur. J. Immunol.* **22**, 2639–2647 (1992).
48. Pannetier, C. *et al*. The sizes of the CDR3 hypervariable regions of the murine T-cell receptor β chains vary as a function of the recombined germ-line segments. *Proc. Natl. Acad. Sci. USA* **90**, 4319–4323 (1993).
49. Casanova, J.L., Romero, P., Widmann, C., Kourilsky, P. & Maryanski, J.L. T cell receptor genes in a series of class I major histocompatibility complex-restricted cytotoxic T lymphocyte clones specific for a *Plasmodium berghei* nonapeptide: implications for T cell allelic exclusion and antigen-specific repertoire. *J. Exp. Med.* **174**, 1371–1383 (1991).
50. Kabsch, W. Automatic processing of rotation diffraction data from crystals of initially unknown symmetry and cell constants. *J. Appl. Cryst.* **26**, 795–800 (1993).
51. Collaborative Computational Project. CCP4 The CCP4 suite: programs for protein crystallography. *Acta Crystallogr. D Biol. Crystallogr.* **50**, 760–763 (1994).
52. Bricogne, G. *et al. autoBUSTER, Version 1.6.0* (Global Phasing, Cambridge, United Kingdom, 2011).
53. DeLano, W.L. *The PyMOL Molecular Graphics System* (DeLano Scientific, San Carlos, California, 2002).